

# Stress Relaxation of Entangled Polymer Networks

Gary S. Grest<sup>a</sup>, Mathias Pütz<sup>b</sup>, Ralf Everaers<sup>c</sup>, and Kurt Kremer<sup>c</sup>

<sup>a</sup>*Sandia National Laboratory, Albuquerque, New Mexico 87185*

<sup>b</sup>*Center for Microengineered Materials, University of New Mexico, Albuquerque, New Mexico 87106*

<sup>c</sup>*Max Planck Institut für Polymerforschung, Postfach 3148, 55021 Mainz, Germany*

The non-linear stress-strain relation for crosslinked polymer networks is studied using molecular dynamics simulations. Previously we demonstrated the importance of trapped entanglements in determining the elastic and relaxational properties of networks. Here we present new results for the stress versus strain for both dry and swollen networks. Models which limit the fluctuations of the network strands like the tube model are shown to describe the stress for both elongation and compression. For swollen networks, the total modulus is found to decrease like  $(V_0/V)^{2/3}$  and goes to the phantom model result only for short strand networks.

## I. INTRODUCTION

Understanding the elastic and relaxation properties of crosslinked networks and rubber has been a longstanding problem [1, 2]. One of the main unresolved issues has been the importance of trapped entanglements in determining the properties of the network. Edwards [3] first introduced the idea that obstacles produced by other chains give rise to a tube in which the monomers of a chain move. Later de Gennes generalized these same ideas to long chains, resulting in the reptation model for the dynamics of an entangled polymer melt [4, 5]. However how entanglements affect the properties of a crosslinked network remains controversial. The reason is twofold. The first is that most experiments do not allow good control of all the microscopic parameters. Second, theoretical descriptions are very complicated due to the presence of quenched disorder and usually contain several adjustable parameters, which are difficult to relate to microscopic details and are almost impossible to determine uniquely from experiment.

Computer simulations can directly address many fundamental questions regarding the dynamics of polymer networks. Details of the microscopic topology, such as the elastically active fraction of the network and loop entanglements, can be identified and controlled. In particular, it is possible to isolate and quantify their effects on macroscopic observables such as the elastic modulus. Simulation results on randomly crosslinked, end-linked [6] and diamond networks [7–9] have conclusively demonstrated the importance of trapped entanglements in determining the elastic and relaxational properties of the network. Results for the mean square displacement of the crosslinks show that they do not move completely freely in space as assumed in the phantom network model but instead are confined to region of space of the order of the tube diameter of an uncrosslinked polymer melt [6]. Further the monomers of strands of length  $N_s > N_e$ , where  $N_e$  is the entanglement length of the melt, are also confined to a tube. The fluctuations of the middle monomers are found to diverge very slowly [6], as  $N_s^{1/2}$  in accordance with reptation theory.

To test the theoretical models, it is advantageous to study model networks, preferably with equal strand lengths between crosslinks and no dangling ends. As such, we have carried out elongation simulations on ideal diamond lattice networks [7–9] and end-linked networks [6]. In the former, the network is constructed to have the coordination of a diamond lattice, with a well controlled topology. A second class of networks, which is not quite as ideal but experimentally realizable is end-linked networks [10, 11]. In this case one starts with a melt of linear chains and adds  $f$ -functional crosslinkers to a fraction of the chain ends. Then by changing the temperature or other conditions, these groups can be activated, so that when another end comes in contact a chemical reaction can occur. We have made a number of model networks following this procedure [6]. A third class which is of high practical importance are randomly crosslinked networks, where crosslinks between melt chains are introduced between any pair of monomers. We have also made model

systems of this type, with the difference that we attached the end-monomers to a randomly chosen nearby monomer resulting in a tri-functional networks instead of the usual four-functional ones. The benefit of this method is that the networks contain no dangling ends which slow down relaxation and are not believed to contribute to zero-frequency stress. Here we present new results for the non-linear stress strain properties of end-linked networks as well as some results on swelling of randomly crosslinked networks.

## II. SIMULATION MODEL

To simulate the networks we use the molecular dynamics method which has been successfully applied to study entanglement effects in polymer melts [12, 13]. In this model the polymers are represented as freely jointed bead-spring chains. All monomeric units of mass  $m$  interact via a purely repulsive Lennard-Jones potential

$$U_{IJ}(r) = \begin{cases} 4\epsilon \left[ \left(\frac{\sigma}{r}\right)^{12} - \left(\frac{\sigma}{r}\right)^6 + \frac{1}{4} \right] & r \leq r_c; \\ 0 & r > r_c, \end{cases} \quad (1)$$

where  $r_c = 2^{1/6}\sigma$ . Monomer units connected along the chain or through the crosslinking procedure are connected by a finite extensible non-linear elastic (FENE) potential. The model parameter are the same as in ref. [12]. The temperature  $T = \epsilon/k_B$ . We use dimensionless units in which  $\sigma = 1$  and  $\epsilon = 1$  and the basic unit of time  $\tau = \sigma(m/\epsilon)^{1/2}$ . The simulations are carried out at a constant density  $\rho = 0.85\sigma^{-3}$ . One of the most important features of this model is that the energy barrier for the crossing of two chain segments is high enough ( $\approx 70k_B T$ ) such that crossing is virtually impossible.

In our previous studies of the mean squared displacement of the chains in a dense melt, we found that the entanglement length  $N_e$  for this model is approximately 35 beads [12]. This result is obtained by comparing the crossover time  $\tau_e$  at which the motion of the monomers in the chain slows down from its initial Rouse-like motion at early times to the slower  $t^{1/4}$  behavior predicted by reptation theory. This result was confirmed by some recent simulations [13] on very long chains ( $N = 350,700$  and  $10000$ ) which also found that the segment motion of the chains was in very good agreement with the reptation model. Estimates from these simulations suggest  $N_e = 32 \pm 2$  [13]. However calculations of the plateau modulus  $G_N^o$ , which were not carried out in our earlier studies due to lack of computer time, indicate that  $N_e$  is much larger. This estimate of  $N_{e,p}$  was obtained using the standard formula of Doi [5]

$$G_N^o = \frac{4}{5} \frac{\rho k_B T}{N_{e,p}}. \quad (2)$$

Depending on the formula we use to fit the non-linear stress strain data, we obtain values for  $N_{e,p}$  between 65 to 80, about twice as large as that obtained from the displacement of the chains. We use the average value 72 when comparing our results to experiment. This suggests an error in the pre-factor  $\frac{4}{5}$  in Eq. 2. Experimentally  $N_e$  is only determined from  $G_N^o$ . We also find that diffusion constant data from the simulations and from experiment agree very well when both are scaled by their Rouse value for short chains and plotted versus  $N/N_{e,p}$  [13].

Here we present results for end-linked systems ( $f = 4$ ) consisting of  $M$  chains of length  $N$ , where  $M/N = 1000/35$ ,  $500/100$ , and  $120/350$ . Due to the slow relaxation and long simulation runs required to obtain the stress at a given strain, the results presented here are for one configuration for  $N = 35$  and  $100$  and two configurations for  $N = 350$ . For comparison we also present results for the plateau modulus for  $N = 350$  and  $N = 700$  [13]. For details of the end crosslinking procedure, see ref. [6]. For the swelling studies, we present results for randomly crosslinked systems ( $f = 3$ ) of size  $M/N/N_s = 500/700/233$  and  $1600/50/18$ , where  $N$  is the melt precursor chain length before crosslinking and  $N_s = N/3$  is the average length of a network strands between crosslinks. We will restrict our analysis to the effect of (partial) swelling in good solvent on the stress-strain relationship of these networks.

### III. NON-LINEAR STRESS STRAIN IN THE DRY STATE

The elastic modulus and non-linear stress versus strain are easily measured experimentally for networks. Numerically the shear modulus can be obtained from uniaxial, volume conserving elongation of the sample which can be described by a diagonal deformation tensor  $\Lambda$  with the stretching factor  $\Lambda_{xx} = \lambda$  and the contraction factors  $\Lambda_{yy} = \Lambda_{zz} = \lambda^{-1/2}$  in the other two directions. The normal stress  $\sigma_N$  is then readily determined from the microscopic virial tensor,  $\sigma_N = \sigma_{xx} - (\sigma_{yy} + \sigma_{zz})/2$ , where  $x$  is the direction of elongation. In the present simulations we vary  $\lambda$  from 2.5 (extension) to 0.5 (compression). Due to finite system size, we are limited to relatively large strains  $\lambda \geq 1.2$  or  $\lambda \leq 0.8$ . For smaller strains, the stress is small and difficult to determine from the noise. After an initial step strain, the strain decays very slowly. For the longest chain lengths studied ( $N_s = 350$ ), runs typically of at least  $10^5\tau$  ( $\leq 2 \times 10^4\tau$  for shorter network strands) were needed to reach equilibrium.

The classical theory of rubber elasticity [1] is based on the empirical fact that the network strands have Gaussian coil statistics. With the exterior deformation described by the tensor  $\Lambda$  the resulting free energy stored in the network strands (of entirely entropic origin) is:

$$F = V \frac{k_B T}{2} \rho_{chain} \left(1 - \frac{2}{f}\right) \sum_{i=1}^3 \Lambda_{ii}^2, \quad (3)$$

where  $V$  is the volume of the sample,  $\rho_{chain}$  the number density of elastically active strands,  $f$  their functionality and  $\Lambda_{ii}$  are the diagonal elements of the deformation tensor. The above result was derived by James and Guth [14] under the assumptions that the crosslinks and the connecting strands are allowed to fluctuate freely without mutual hindrance of each other (this is commonly referred to as the phantom chain model). If one fixes the crosslinks in space so that they deform affinely under strain (the affine model) the factor  $(1 - 2/f)$  disappears and one arrives at the old result given by Kuhn [15]. With this one can readily derive an expression for the normal tension in the sample as function of the elongation [16],

$$\sigma_N = -\frac{\lambda}{L^2} \frac{dF(\lambda)}{d\lambda} = \rho_{chain} k_B T \left(1 - \frac{2}{f}\right) \left(\lambda^2 - \frac{1}{\lambda}\right), \quad (4)$$

where  $L^2/\lambda$  is the transversal cross section of the sample. Flory and Erman [17,18] extended the theory to allow entanglement effects on the crosslinks by reducing their fluctuation radii, thus interpolating between the affine and the phantom model with a more complicated stress strain behavior. The model is quite successful describing many experimental stress-strain relations as well as our data (see Fig. 1a). However, due to our additional knowledge on the conformations of the chain [6], we know that the fluctuations of the entire chains are restricted and therefore we think that constraint models for junctions alone should be discarded. Many models exist which limit the fluctuations of the network strands like the tube-model by Heinrich *et al.* [19] or some recent constraint models by Kloczkowski *et al.* [20], Rubinstein and Panyukov (RP) [21,22] and Everaers [23]. Of these, especially the RP model is rather appealing, since it introduces only one additional parameter, the chain length between entanglements  $N_e$ . Erman's and Everaers' recent models introduce a large set of constraint parameters and little is known yet how to choose them, although the physical meaning of these parameters is relatively clear. At least for Everaers' model it has been demonstrated how to obtain more detailed knowledge about network fluctuations by measuring these parameters directly through simulations of highly idealized networks with diamond lattice topology [9].

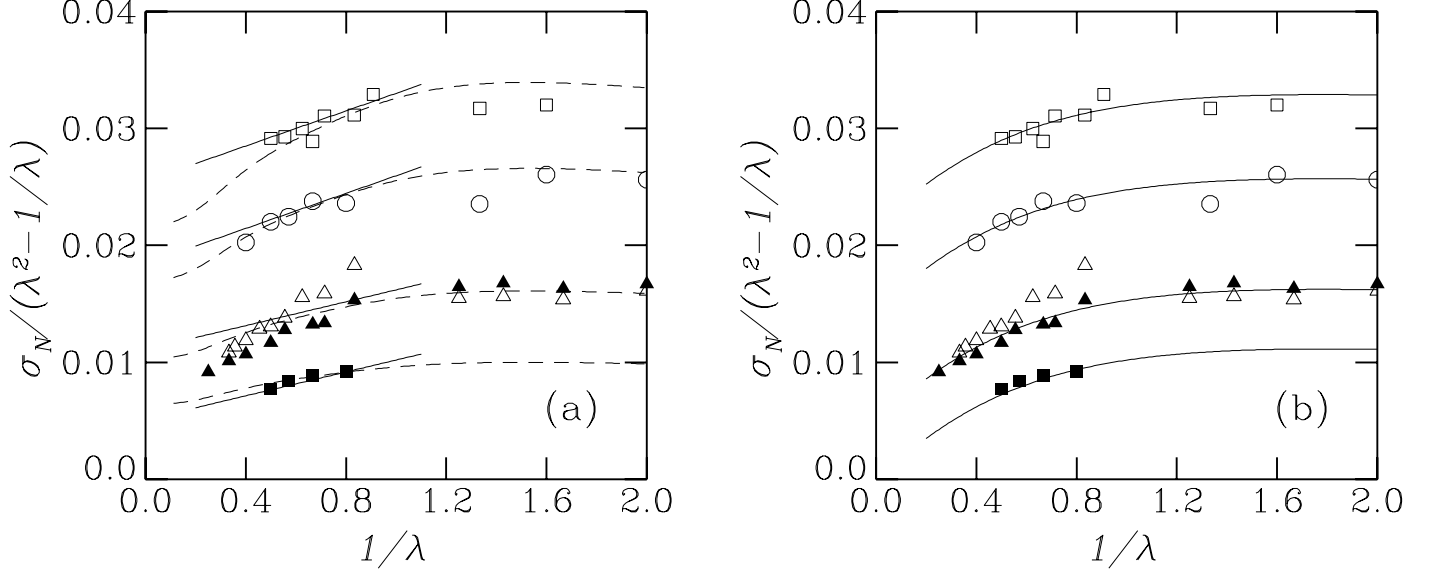


FIG. 1. Stress-strain relation for end crosslinked networks compared to (a) the Mooney-Rivlin, Eq. 7 (solid lines), and constrained junction (non-affine deformation parameter  $\kappa = 5.0$ ) [17] (dashed lines) models and (b) the Rubinstein-Panyukov form, Eq. (6). Data are for  $N_s = 35$  ( $\square$ ), 100 ( $\circ$ ) and 350 (triangles). Also shown is the plateau value for an uncrosslinked melt of chains of length  $N = 700$  ( $\blacksquare$ ).

An analysis of the type presented in [9] is beyond the scope of this paper and we shall limit our analysis along the lines of the RP model which has an extra entanglement term in the free energy:

$$F_e = \frac{1}{2} V G_e \sum_{i=1}^3 \left( \Lambda_i + \frac{1}{\Lambda_i} \right). \quad (5)$$

It is customary to renormalize the stress  $\sigma_N$  by the classical functional dependence on  $\lambda$ ,  $\sigma_N^* = \sigma_N / (\lambda^2 - 1/\lambda)$  to emphasize deviations from this behavior. Together with some recent improvement [22] on the theory which takes into account reorganization of the constraining tubes due to anisotropic tube deformations [21] this additional term results in a stress-strain relation for uniaxial strain:

$$\sigma_N^* = G_c + 1.84 G_e / (\lambda + 0.84 \lambda^{-1/2}) \quad (6)$$

In Fig. 1 we show the stress-strain curves for our various model end-linked networks together with fits to Eq. 6 to the semi-empirical Mooney-Rivlin [1] formula

$$\sigma_N^* = 2C_1 + 2C_2/\lambda \quad (7)$$

and to the resulting stress-strain relation of the theory of Flory and Erman (formula not shown due to complexity) for comparison. We can see that the elongation branch can be described by each of these equations, while the Mooney-Rivlin form provides a clearly inadequate description of the compression data. Note, that the stress has been normalized by the classical stress dependence (Eq. 4) on  $\lambda$ , so that deviations from the classical behavior are more clearly visible.

However a more quantitative analysis of the resulting fit-parameters shows that the situation is less conclusive. We performed two fits to the PR model. For the first fit the value of  $G_e$  was determined from the plateau modulus for the uncrosslinked melt of free chains and was held fixed. Using the RP form,  $G_e = 0.0102\epsilon/\sigma^{-3}$ , while  $G_c = 0.0145$ , 0.0097, and 0.0034 $\epsilon/\sigma^{-3}$  for  $N_s = 35$ , 100 and 350, respectively. If

$G_c$  is equivalent to either phantom or affine results the values of  $G_c(N_s)$  should scale with the crosslink density ( $N_s^{-1}$ ). The values for the ratios  $G_c(35)/G_c(350) = 4.3$  and  $G_c(100)/G_c(350) = 2.9$ , compared to the phantom/affine prediction of 10 and 3.5. The absolute values for  $G_c$  generally appear too high compared to the phantom and/or the affine results. A different way to look at the results is to set  $G_c$  to their expected values and fit  $G_e$ . For our shortest strand network  $N_s = 35$ , fluctuations of the crosslinks are of the order the radius of gyration of the entire chain, hence we expect  $G_c$  should equal its value for the phantom model,  $G_c = 0.012\epsilon/\sigma^{-3}$ . Using this value for  $G_c$ , we find  $G_e = 0.0014\epsilon/\sigma^{-3}$ . For our  $N_s = 350$  networks the crosslinks explore much less space than the radius of gyration of the whole chain, thus the behavior is expected to be more in accordance with the affine model,  $G_c = 0.0022\epsilon/\sigma^{-3}$  (after adjusting for the fact that 10 of 120 chains are not elastically active). Using this value for  $G_c$  we find  $G_e = 0.0012\epsilon/\sigma^{-3}$ . Thus the effective  $G_e$  becomes larger as the chains become shorter, i.e. the presence of more crosslinks provides stronger constraints as in the melt case. A more rigorous test of the RP model would be to compare networks of strand lengths  $N_s = 350$  and 700, which is beyond the amount of available computer time at present. However experimentally the more relevant region in parameter space lies in the range  $N = 35$  to  $N = 350$  since it is difficult to make networks with very large strand lengths.

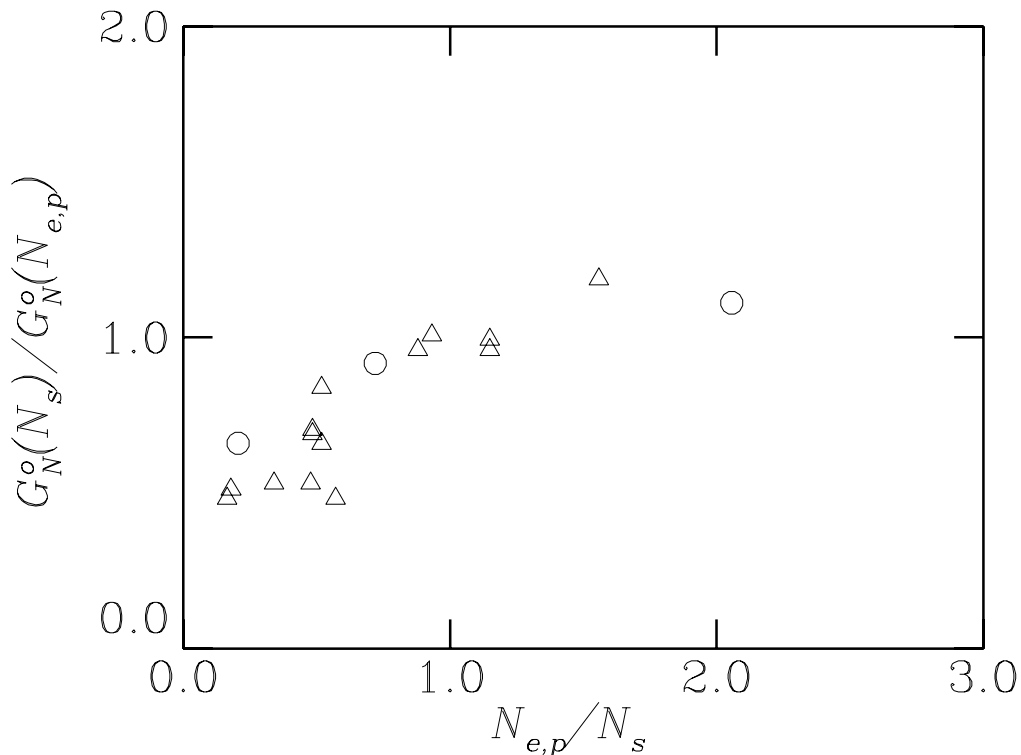


FIG. 2. Plot of modulus for end linked networks from simulation ( $\circ$ ) and experiment ( $\triangle$ ). The modulus has been normalized by its value at  $N_e$ . The experimental data for  $G_N^o(M_s)$  of PDMS networks are from Patel *et al.* [11].

The elastic modulus  $G_N^o$  can be obtained from extrapolating the slope of the non-linear stress-strain curves to  $\lambda = 1$ . Results for  $G_N^o$  are shown in Fig. 1 using the RP form to extrapolate to  $\lambda = 1$ . The MR form gives larger values for  $G_N^o$ . To compare to experimental data for PDMS end-linked networks, we have normalized the modulus for its value at  $N_{e,p} = 72$ . For PDMS the entanglement molecular weight  $M_{e,p} = 9600$ . As seen from Fig. 1, our simulation results agree with experiment. The large scatter in the experimental data for strand lengths  $N_s \gtrsim 2 \cdot N_{e,p}$  shows the difficulty to create good networks with the endlinking method.

#### IV. SWOLLEN NETWORKS

Experimental results [24, 25] show that the entanglement contribution to the modulus decreases significantly if the networks are swollen in good solvent. To investigate this effect we let our randomly crosslinked networks swell in vacuum. Since our model only involves repulsive interactions vacuum acts as a perfect solvent for our model networks. At various degrees of (incomplete) swelling we performed stress-strain experiments (only elongation) with two of our swollen samples. We used formula (6) to fit the resulting set of stress-strain curves and estimate the modulus, though for extracting the modulus any of the forms for  $\sigma_N$  could have been used. Fig. 3 shows the stress-strain relations for the unswollen states and at equilibrium swelling (when elastic free energy and entropy of dilution cancel each other). The swollen systems show the empirically expected behavior of classical rubber elasticity (4) which becomes clearer when one looks at the classical and entanglement contributions to the modulus shown in Tab. I. These were determined by fits to Eq. (6). One can see from the table as well as from Fig 3. that the total modulus (slope of the curves for  $\lambda \rightarrow 1$ ) approximately decreases like  $q^{-2} = (V_0/V)^{2/3}$ . For the short strand network  $N_s = 18$  it is nice to see that the system recovers the phantom result at maximum swelling (the effective values for  $G_c$  and  $G_e$  are no longer meaningful, since finite chain length effects become very important at high swelling and large deformations which are not accounted for in the theory, but still they are useful to extract a total modulus). For the long chain a entanglement contribution remains, however it is shifted over into  $G_c$  which is still about a factor of 1.5 to 4 larger than the affine and phantom values, respectively). If RP theory is applied to swelling, in the spirit of Flory and co-workers (i.e. assuming that the statistics of the chains remains Gaussian with swelling), this theory (as well as others) actually predicts, that the entanglement contribution should vanish and the classical crosslink contribution should remain constant which qualitatively agrees with our findings.

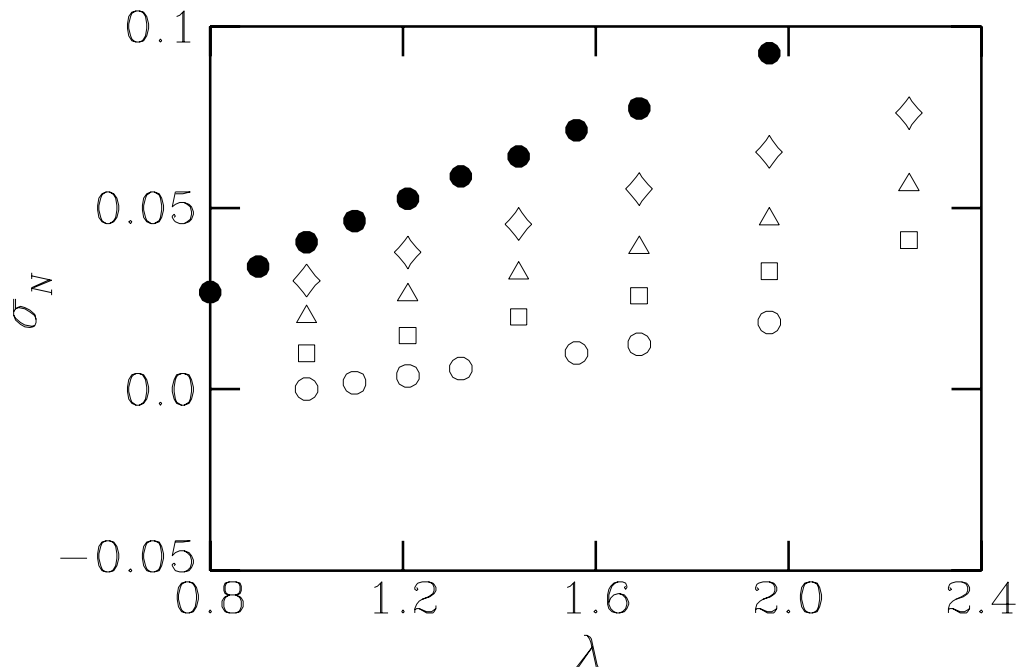


FIG. 3. Stress-strain relations for a randomly crosslinked three-functional system of average strand length  $N_s = 233$  for various degrees of swelling:  $q = 1.0$  ( $\bullet$ ),  $q = 1.2$  ( $\diamond$ ),  $q = 1.4$  ( $\triangle$ ),  $q = 1.6$  ( $\square$ ),  $q = 1.9$  ( $\circ$ ). For clarity the curves are shifted in y-direction by  $0.01\epsilon/\sigma^3$  with respect to each other.

This follows from a simple analysis of the leading powers in  $\lambda$  of the different contributions to the free energy. Let us split up the deformation into an isotropic swelling factor  $q$  and an anisotropic deformation  $\Lambda'_{ii} : \Lambda_{ii} = q\Lambda'_{ii}$ . The free energy due to crosslinks is then proportional to  $q^2$ , but the system size  $L$  also changes proportional to  $q$ . Therefore the powers of  $q$  in the formula for the stress cancel exactly. The entanglement contribution in the RP model is proportional to the first power of  $q$  only and thus its stress contribution should decrease like  $1/q$ , whereas we find it behaves more like  $q^{-2}$  for our networks. The most important key to understand this behavior certainly lies in the non-Gaussian statistics of the swollen chains. We recently found, that the fractal structure of the chains changes significantly under swelling and can be described as random walks only on length scales beyond the entanglement length  $N_e$  and below can be described by a fractal exponent of  $\nu \approx 0.7$  [26], which is in disagreement with the widely assumed single chain good solvent exponent  $\nu \simeq 3/5$ . Further our results for long-chain networks seem to favor a form of the free energy where the entanglement contribution behaves approximately like  $F_e(q, \lambda) \rightarrow G(N_s) \cdot F_c(\lambda)$  for large  $q$ . Loosely speaking, the trapped entanglements behave more like physical crosslinks for high swelling.

$N_s$	$G_{ph}$	$q$	$G_c$	$G_e$	$G_{tot}$
233	0.0012	1.0	0.0102(05)	0.0110(10)	0.0212(15)
		1.2	0.0074(06)	0.0058(10)	0.0132(16)
		1.4	0.0062(05)	0.0037(02)	0.0194(12)
		1.6	0.0059(03)	0.0018(04)	0.0077(07)
		1.9	0.0058(05)	-0.0005(05)	0.0053(10)
18	0.017	1.0	0.0190(20)	0.0120(20)	0.0310(40)
		1.2	0.0254(60)	-0.0047(60)	0.021(12)
		1.3	0.0327(30)	-0.0166(30)	0.0161(60)
		1.4	0.0314(12)	-0.0162(15)	0.0151(27)

TABLE I. Classical crosslink ( $G_c$ ) and entanglement ( $G_e$ ) contributions to the total modulus  $G_{tot}$  in swollen ( $q^3 = V/V_0$ ) randomly crosslinked three-functional systems of average strand length  $N_s$ . Here  $G_{ph} = \rho_{chain}(1-2/f)$  with  $f = 3$  is the modulus predicted by the phantom model (3). Errors in parenthesis are those obtained by the non-linear fit.

## V. CONCLUSION

In this paper we have presented molecular dynamics simulation results for the non-linear stress strain properties of a crosslinked polymer network. Because the topology of the network can be readily controlled in the simulations, computer simulations provide a powerful way to test various theoretical models. Combined with our earlier studies, we are now beginning to obtain a better microscopic understanding of how the topology of the network controls the dynamics and relaxation of the chain segments and the crosslinks. All of our data strongly support constraint models in which the monomers are constrained to move in a tube formed by the neighboring chains. The crosslinking process traps in the dynamic entanglements present in the uncrosslinked melt. These trapped entanglements dominate the stress relaxation and modulus when the strand length between crosslinks is large. In the unswollen, dry state, the chains are Gaussian in agreement with all models. However as the system is swollen in a good solvent, they become strongly non-Gaussian on length scales less than the distance between crosslinks. In the dry state, a number of model for the stress-strain relation can be used to describe the data, although further work is necessary to arrive at a more quantitative understanding physical of the resulting fitting parameters. Clearly a more microscopic approach investigating network fluctuations is necessary to distinguish between these models. In the swollen state we find that short stranded networks eventually recover the phantom result for the modulus, however finite chain length corrections and a proper account for the non-Gaussian statistics are clearly needed to describe their entire ( $\lambda \neq 1$ ) stress-strain relations. In long strand networks the entanglement contribution to the modulus decreases with swelling but compared to the predictions of the phantom and affine models a significant contribution remains. The stress strain curves at high swelling are better described by classical (crosslinks only) theories, hence the remaining effect of entanglements appears more like an additional crosslink contribution.

## Acknowledgments

Sandia is a multiprogram laboratory operated by Sandia Corporation, a Lockheed Martin Company, for the United States Department of Energy under Contract DE-AC04-94AL85000.

- 
- [1] L. R. G. Treloar, *The Physics of Rubber Elasticity* (Clarendon, Oxford, 1975).
  - [2] W. W. Graessley, *Adv. Polym. Sci.* **47**, 67 (1982).
  - [3] S. F. Edwards, *Proc. Phys. Soc.* **92**, 9 (1967).
  - [4] P. G. de Gennes, *Scaling Concepts in Polymer Physics* (Cornell University Press, Ithaca NY, 1979).
  - [5] M. Doi and S. F. Edwards, *The Theory of Polymer Dynamics* (Clarendon, Oxford, 1986).
  - [6] E. R. Duering, K. Kremer, and G. S. Grest, *J. Chem. Phys.* **101**, 8169 (1994). In this paper a mode analysis was used to determine the modulus  $G_N^o$ . However the formulation used was incorrect. Though the qualitative features of the modulus with strand length  $N_s$  were correct, the results were not quantitative. In particular the factor  $A^o$  relating  $G_N^o$  to that determined from the mode analysis was incorrect. This will be discussed in more detail in a forthcoming paper.
  - [7] R. Everaers and K. Kremer, *Macromolecules* **28**, 7291 (1995).
  - [8] R. Everaers and K. Kremer, *Phys. Rev. E* **53**, R37 (1996).
  - [9] R. Everaers, *New J. Phys.* **1**, 12.1 (1999).
  - [10] J. P. Queslel and J. E. Mark, *Adv. Polym. Sci.* **65**, 135 (1984).
  - [11] S. K. Patel *et al.*, *Macromolecules* **25**, 5241 (1992).

- [12] K. Kremer and G. S. Grest, *J. Chem. Phys.* **92**, 5057 (1990).
- [13] M. Pütz, K. Kremer, and G. S. Grest, submitted / xxx.lanl.gov preprint: cond-mat/9906204 (1999).
- [14] H. James and E. Guth, *J. Chem. Phys.* **15**, 669 (1947); **21**, 1039 (1953).
- [15] W. Kuhn, *J. Polymer Sci.* **1**, 380 (1946).
- [16] Note, that most experimentalists define the normal stress as the force per unstretched crosssection, thus the extra factor of  $\lambda$  disappears. In simulations we use the given definition since that corresponds to the definition from the microscopic virial tensor.
- [17] P. J. Flory, *J. Chem. Phys.* **66**, 5720 (1977).
- [18] B. Erman and P. J. Flory, *J. Chem. Phys.* **68**, 5363 (1978).
- [19] G. Heinrich, E. Straube, and G. Helmis, *Adv. Polym. Sci.* **85**, 33 (1988).
- [20] A. Kloczkowski, J. E. Mark, and B. Erman, *Macromolecules* **28**, 5089 (1995).
- [21] M. Rubinstein and S. Panyukov, *Macromolecules* **30**, 8036 (1997).
- [22] M. Rubinstein and S. Panyukov (private communication, 1999).
- [23] R. Everaers, *Eur. Phys. J. B* **4**, 341 (1998).
- [24] J. E. Mark, *Rubber Chem. Tech.* **48**, 495 (1975).
- [25] S. P. Obukhov, R. Colby, and M. Rubinstein, *Macromolecules* **27**, 3191 (1994).
- [26] M. Pütz, R. Everaers, and K. Kremer, to be published in *Phys. Rev. Lett.* / xxx.lanl.gov preprint: cond-mat/9909453 (1999).